2D nonlinear Acoustic Wave equation in heterogeneous fluid

Renan A. Peres[1], Antônio M. F. Frasson[1], Carlos F. Loeffler[2], Fábio P. Piccoli[1], Julio T. A. Chacaltana[1]

[1] *Postgraduate Program in Environmental Engineering, Federal University of Espírito Santo*
Avenida Fernando Ferrari, 514,Goiabeiras, 29075-910, Espírito Santo, Brazil
renan.peres@edu.ufes.br, antonio.frasson@ufes.br, fabio.p.piccoli@gmail.com, julio.chacaltana@ufes.br
[2] *Postgraduate Program in Mechanical Engineering, Federal University of Espírito Santo*
Avenida Fernando Ferrari, 514,Goiabeiras, 29075-910, Espírito Santo, Brazil
carlosloeffler@bol.com.br

Abstract. The nonlinear acoustic wave equation with source term of the P-wave propagation in heterogeneous fluid (Chacaltana [1], Peres [2]) is extended and solved numerically by the Finite Element Method (FEM). To minimize the residue in each element, the Weighted Residual Method (Petrov-Galerkin) is used. Linear and parabolic basis interpolation functions are implemented. A Ricker-type source (Chacaltana [1]; Picolli [3]) is used to generate the P-wave. The Neumann reflective (natural) and non-reflective ABC (Absorbing Boundary Condition) boundary conditions, presented in Frasson [4], were implemented and tested in rectangular and circular domains. The numerical code is written in Fortran 95 language and the Octave graphical interface is used to analyze the results. The GMSH mesh generator (v. 4.8.4) is used to represent the continuous domain by a set of discrete points that group together forming a non-uniform mesh of triangular elements. Numerical tests are carried out to verify the maintenance of symmetry after multiple reflections and the effectiveness of 1st and 2nd order ABC. The numerical results show a good agreement with existing results in the literature.

Keywords: Non-linear Equation of Acoustic Wave; Heterogeneous fluid; Finite Element Method; Ricker wavelet.

1 Introduction

Understanding the transformations of the P-wave during its propagation in heterogeneous media is of greatest importance in different areas of science. Linear modeling for P-wave propagation in homogeneous and heterogeneous media has been addressed by several authors (Chacaltana [1]; Picolli [3]; Araujo [5]; Costa [6]; Valente [7]; Neto [8]). However, the non-linear modeling of the P-wave in a heterogeneous medium is still a challenge, particularly when it comes to finding analytical solutions and developing boundary conditions that allow the wave to exit without causing reflection. Acoustic nonlinearity has been a focus of investigation since the last century. Among the researchers, Fubini-Ghiron (*apud* Campos-Pozuelo [9]) proposed an explicit solution for progressive plane waves. Later, analytical models for cylindrical and spherical waves were developed by Blackstock [10]. Comprehensive reviews on the development of acoustic wave nonlinearity can be found in Beyer [11], Lauterborn [12], Pierce [13] and Garrett [14]. Hamilton & Blackstock [15] presented analytical approximations to describe the nonlinear behavior of plane waves.

Assuming that the understanding of Acoustic Wave propagation becomes increasingly refined by considering the nonlinearity of acoustic phenomena, the present work aimed to derive and numerically solve the 2D non-linear Acoustic Wave equation for heterogeneous fluid media (Chacaltana [1]; Peres [2]) using the Finite Element Method (FEM) combined with the Weighted Residuals Method (Petrov-Galerkin) and test the performance of the 1st and 2nd order ABC boundary condition. A Ricker-type source was used (Picolli [3]). The 2D mesh, composed of first-order triangular elements, was generated using the GMSH mesher (v. 4.8.4), and Neumann and ABC boundary conditions (Bamberger [16]; Frasson, [4]) were implemented. The results are presented, and the performance of the 1st and 2nd order ABC, applied to the nonlinear solution of the acoustic wave, is discussed. This work expands the 1D modeling presented in Peres [2] to a 2D modeling, to investigate the propagation of the P-wave in a non-homogeneous medium considering the effects of nonlinearity in the modeling. The improvement and development of the computational code is tested to verify the symmetry imposed by the geometry and to investigate the influence of open boundary conditions. As an initial step towards understanding the propagation of the P-wave, for example, in seismic oil exploration, in understanding the Earth's interior and in the health area for the technological development of processes such as ultrasonography. This work verifies the maintenance of symmetry after multiple reflections and the effectiveness of 1st and 2nd order ABCs in square and circular geometries.

2 Nonlinear acoustic wave equation for an inhomogeneous fluid

The acoustic wave, also known as pressure wave (P-wave), is a mechanical wave that is related to the pressure variation in the medium caused by a mechanical disturbance. The equation for the propagation of the P-wave in a compressible fluid is deduced from the laws of fluid mechanics and the principles of thermodynamics. Following Chacaltana [1] and Piccoli [2], for a compressible fluid and an isentropic process, the equations representing conservation of mass, conservation of momentum, and the equation of state can be written, respectively, in the mixed form as:

$$\frac{d\rho}{dt}+\rho\nabla.\vec{u}=\dot{M} \tag{1}$$

$$\rho\frac{du}{dt}=-\nabla p \tag{2}$$

$$E=\rho c^2 \tag{3}$$

Where c $\left|c^2=(\frac{\partial p}{\partial \rho})_s\right|$ is the P-wave velocity during the isentropic process, while E $\left|E=\rho\frac{dp}{d\rho}\right|$ is the fluid's compressibility modulus, which describes the expansion (contraction) behavior of a small volume of fluid due to a decrease (increase) in pressure (Lauterborn [12]), where ρ stands for the specific mass, p for the pressure field, u for the velocity field and $\dot{M}$ acts as a mass source. Using the definition of the compressibility modulus, equations (1) and (2) can be written in non-conservative form as

$$\frac{\rho}{E}[\frac{\partial p}{\partial t}+(\vec{u}.\nabla)p]+\rho\nabla.\vec{u}=\dot{M} \tag{4}$$

$$\frac{\partial\vec{u}}{\partial t}+(\vec{u}.\nabla)\vec{u}=-\frac{1}{\rho}\nabla p \tag{5}$$

By deriving equation (4) in relation to time, rearranging and making use of equation (5), the equation for pressure is obtained after manipulation, as long as the fluid velocity is known.

$$\frac{\partial^2 p}{\partial t^2}+\frac{\partial}{\partial t}(\vec{u}.\nabla p)-\rho c^2\nabla.(\frac{1}{\rho}\nabla p)-\rho c^2\nabla.(\vec{u}.\nabla\vec{u})=\ddot{P}_f \tag{6}$$

When obtaining equation (6) it is considered that the compressibility modulus E (ρc^2) does not vary with time but can vary in space. For a homogeneous fluid, equation (6) reduces to the classical wave form if the non-linear terms are disregarded and there is no pressure source term, $\ddot{P}_f$.

2.1 Initial and Boundary Conditions

In dynamic problems that evolve over time there is a need to provide initial conditions. Two initial conditions are provided for pressure and one initial condition for velocity, and they refer to the fact that there is no velocity induced by pressure if it is zero at these 2 instants of time. The initial conditions for equations (5) and (6) at time $t\leqslant t_0$ are:

$$\vec{u}(x,y,t_0)=\vec{u_0}=0 \text{ and } p(x,y,t_0)=p_0=0 \tag{7}$$

$$p(x,y,t)=0 \text{ for all } t<t_0 \tag{8}$$

Two types of boundary conditions are implemented, the (natural) Neumann boundary condition which causes a perfect reflection when the Neumann condition is equal to zero at the boundary.

$$\nabla p.\hat{n}=0 \tag{9}$$

And, the 1st and 2nd order ABC, Frasson [4], to radiate the waves outside the domain.

$$\nabla p.\hat{n}+\frac{1}{c}\frac{\partial p}{\partial t}=0 \tag{10}$$

$$\frac{\partial(\nabla p.\hat{n})}{\partial t}+\frac{1}{c}\frac{\partial^2 p}{\partial t^2}-\frac{c}{2}\nabla^2_{\tan}p=0 \tag{11}$$

For the corner boundary condition, the formulation proposed in Bamgerger [16] was implemented.

$$\frac{\alpha}{c}\frac{\partial p}{\partial t}+\frac{\partial p}{\partial x}+\frac{\partial p}{\partial y}=0 \tag{12}$$

where α = 3/2.

2.2 Source term

To generate the acoustic wave, a Ricker-type source (Piccoli [2]) was used. This source is made up of a pulse characterized as "Mexican hat", obtained from the second derivative of the Gaussian function.

$$\ddot{P}_f(t) = t_0 e^{(-0.25\pi f_c^2 t_0^2)} \tag{13}$$

Here $t_0 = t - \frac{2\sqrt{\pi}}{f}$ is the time for the generated pulse and f_c is the central frequency, defined in terms of the cutoff frequency f, $f_c = 3\sqrt{f}$. This source was chosen due to its simple shape and implementation, helping in the interpretation of the results. The smoothing provided at the beginning of the simulation avoids numerical noise and wave distortions. In addition, to being widely used in seismic, since it is very effective in describing the signal spectrum as a linear combination of the Ricker wavelet spectra (Gholamy [17]; Wang [18]).

2.3 Stability Criterion

To guarantee the numerical stability of the model, the criterion as proposed by Oden [19] for non-linear hyperbolic equations was considered. Where h is the element size and c_{max} is the maximum wave speed.

$$\Delta t < \frac{\sqrt{2}h}{2c_{max}} \tag{14}$$

3 Finite Element Method

To achieve the numerical solution of the non-linear Acoustic Wave equation (6), the equation of motion (5) is solved together. Both are solved in the same time loop, in such a way that the equation of motion (5) is first solved so that the values of u and v become known in the solution of the wave equation (6). And consequently, the pressure gradient becomes known to solve the equation of motion (5) in the next time step. For the discretization process, FEM and Weighted Residual Method (Petrov-Galerkin) are applied through the development of the product with weight functions w and solved the inner product over the entire 2D domain.

$$< \frac{\partial \vec{u}}{\partial t}, w > = < -\frac{1}{\rho}\nabla p, w > - < \vec{u}.\nabla \vec{u}, w > \tag{15}$$

$$\int_s w \frac{\partial \vec{u}}{\partial t} ds = -\int_s w \frac{1}{\rho}\nabla p \, ds - \int_s w \vec{u}.\nabla \vec{u} ds \tag{16}$$

On the right side of equation (16), there is the term referring to the pressure gradient, which is calculated by equation (6) and the advective term, representing nonlinearity. The nonlinearity is worked in such a way as to bring it closer to a linear system considering u and v of the previous time step "n-1". Therefore, the shorter the time interval for each time step, the better the approximation tends to be.

$$\frac{\partial}{\partial t}\int_s w \vec{u} \, ds = -\int_s \nabla p^{n-1} \frac{w}{\rho} ds - \int_s w(u^{n-1}\frac{\partial}{\partial x} + v^{n-1}\frac{\partial}{\partial y})\vec{u} \, ds \tag{17}$$

Having applied the Weighted Residuals Method (Petrov-Galerkin), it is considered that the weight function w (N_i) has the same value as the approximation basis function from the FEM (N_j).

$$\frac{\partial}{\partial t}\sum_{j=1}^{n} u_i \int_s N_i N_j ds = -\sum_{j=1}^{n} p_j^{n-1} \int_s \frac{N_i}{\rho}\frac{\partial N_j}{\partial x} ds - \sum_{j=1}^{n} u_j \int_s (u^{n-1} N_i \frac{\partial N_j}{\partial x} + v^{n-1} N_i \frac{\partial N_j}{\partial y}) ds \tag{18}$$

$$\frac{\partial}{\partial t}\sum_{j=1}^{n} v_i \int_s N_i N_j ds = -\sum_{j=1}^{n} P_j \int_s \frac{N_i}{\rho}\frac{\partial N_j}{\partial y} ds - \sum_{j=1}^{n} v_j \int_s (u N_i \frac{\partial N_j}{\partial x} + v N_i \frac{\partial N_j}{\partial y}) ds \tag{19}$$

Where n in sum is the number of nodes. To discretize the temporal derivative, the backward finite difference method was used. Thus, we arrive at the components of the equation of motion in discrete form:

$$\frac{\{u\}^n - \{u\}^{n-1}}{\Delta t}\int_s N_i N_j ds = -\{p\}^{n-1}\int_s \frac{N_i}{\rho}\frac{\partial N_j}{\partial x} ds - \{u\}^{n-1}\int_s (u^{n-1} N_i \frac{\partial N_j}{\partial x} + v^{n-1} N_i \frac{\partial N_j}{\partial y}) ds \tag{20}$$

$$\frac{\{v\}^n - \{v\}^{n-1}}{\Delta t}\int_s N_i N_j ds = -\{p\}^{n-1}\int_s \frac{N_i}{\rho}\frac{\partial N_j}{\partial y} ds - \{v\}^{n-1}\int_s (u^{n-1} N_i \frac{\partial N_j}{\partial x} + v^{n-1} N_i \frac{\partial N_j}{\partial y}) ds \tag{21}$$

In matrix form, the final discrete form of the equation of motion (22) and (23) is expressed.

$$\{u\}^n[Mu] = -(\{P\}^{n-1}[Reu] - \{u\}^{n-1}[Mdu])\Delta t + \{u\}^{n-1}[Mu] \tag{22}$$

$$\{v\}^n[Mu] = -(\{P\}^{n-1}[Rev] - \{v\}^{n-1}[Mdv])\Delta t + \{v\}^{n-1}[Mu] \tag{23}$$

Where the matrix *[Mdu]* and *[Mdu]* represents the non-linearity of the equation of motion. The same procedure was applied to the nonlinear acoustic wave equation (6), and the final form was achieved (24).

$$\{P\}^{n+1}[M]=\frac{\Delta t^2 P_f}{\rho}-\Delta t^2[K]\{P\}^n+2[M]\{P\}^n-[M]\{P\}^{n-1}-[\Delta t[D]\{P\}^n+\Delta t[D]\{P\}^{n-1}-\Delta t^2[Kd]\{u+v\}^n] \quad (24)$$

Where the matrices *[D]* and *[Kd]* represent the non-linearity of the equation, that is, they depend on the induced velocity components *u* and *v* calculated through equations (22) and (23).

4 Test Cases

The discrete Finite Element model has been developed by the authors of this work. The code was written in Fortran 95 language. Five tests were developed to evaluate the numerical model and the ABC boundary conditions. The first test aims to evaluate the symmetry of the results after multiple reflections of the P-wave in a square geometry, with the generation of the P-wave in the geometric center. In Test 2, the same square geometry is used, with the source at the geometric center. The test aims to evaluate the first and second order absorbing boundary conditions using the linear and non-linear formulation of P-wave propagation. Test 3 considers a rectangular geometry composed of two layers with different physical properties. The objective here is to evaluate the reflection of the wave when it is propagating from one medium to another. In Test 4, P-wave propagation is performed with the nonlinear model in a square geometry to compare the effectiveness of the first and second order absorbing boundary condition and the interaction of the P-wave with the corners. Finally, Test 5 has the same purpose as Test 4, but is carried out in a circular geometry. Test data can be seen in Table 1. For all cases, the mesh was constructed using first-order triangular elements of 10m and the time interval was 10^{-3}s.

Table 1. Parameters used in the five tests for the propagation of the P-wave generated by a pressure source.

Parameters	**Test 1**	**Test 2**	**Test 3**	**Test 4**	**Test 5**
Mesh gemometry	Square	Square	Square	Square	Circular
Boundary Condition	Neumann	2nd order ABC	2nd order ABC	1st & 2nd ABC	1st & 2nd ABC
f_c	30Hz	30Hz	30Hz	30Hz	30Hz
Dimensions	500mx500m	500mx500m	800mx500m	500mx500m	500m
x_f / y_f	250m/250m	250m/250m	200-500m/250m	250m/250m	250m/250m
c_{max}	1500m/s	1500m/s	3000m/s	1500m/s	1500m/s
c_{min}	1500m/s	1500m/s	1500m/s	1500m/s	1500m/s
dt	10^{-3} s	10^{-3} s	10^{-3} s	10^{-3} s	10^{-3} s

5 Results and Discussion

In Test 1, the total reflection of the nonlinear acoustic wave with the expected symmetry was verified (Figure 1). The Neumann condition satisfactorily simulated a rigid wall, causing the peak to reflect as a peak and the trough as a trough. At t = 0.556s (a), we see wavefront that have just reflected off the wall and are already returning. By t = 1s (b), the reflections have interacted with each other multiple times, forming the symmetrical pattern in question. A seismogram was also generated to better visualize the reflections, capturing the lateral and frontal reflections based on the pressures measured along a line intersecting the source. The pulse is generated around t = 0.3s, reaching the edge around t = 0.5s. From this moment on, multiple reflections can be observed, indicated below the dashed red line (c).

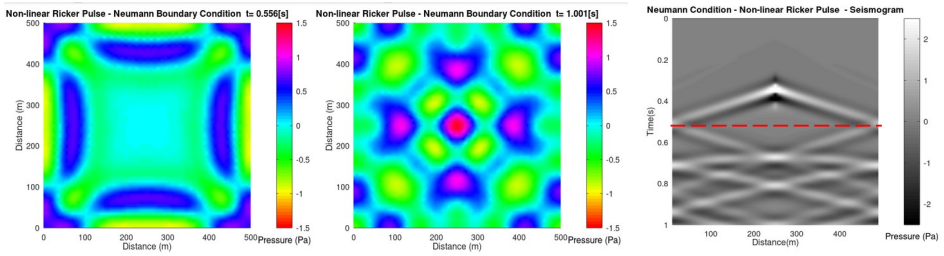

Figure 1. Non-linear acoustic wave propagation with Neumann condition (rigid wall) at t = 0.556s (a) and t = 1s (b). In (c), we have the seismogram.

In Test 2, no significant difference was detected in the application of the second-order ABC to the linear and nonlinear solutions of the acoustic wave (Figure 2). This result is attributed to the low magnitude of nonlinearity compared to the simulated pressure, given that the acoustic pulse induced a velocity on the order of 10^{-7}m/s. This occurs because the formulation used takes into account the small amplitude theory, resulting in the non-linearity having a very small effect. The efficiency of the second-order ABC proved to be satisfactory for both solutions.

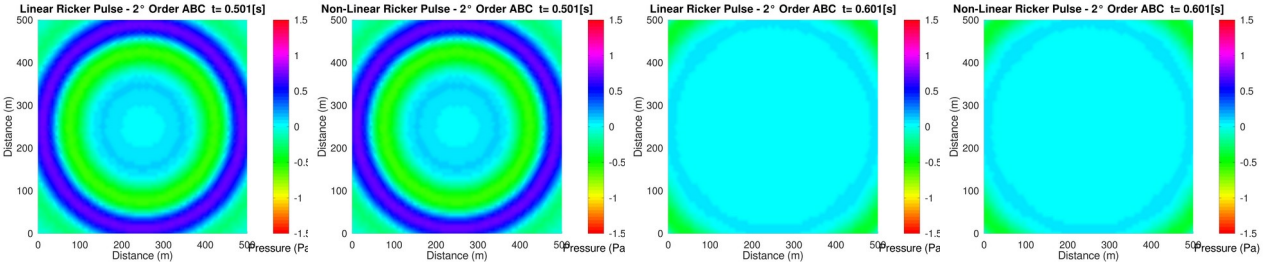

Figure 2. Linear and non-linear acoustic wave propagation with 2nd order ABC (Absorbing Condition).

In Test 3, the pressure source was positioned in two distinct regions of the mesh: x_f=200m and x_f=500m. In the simulation for x_f=500m, the domain was divided into two layers: ρ_1=1000kg/m^3 (0 to 200m) and ρ_2=2500kg/m^3 (200m to 800m). In the second, where x_f=200m, the domain was divided into ρ_1=1000kg/m^3 (0 to 400m) and ρ_2=2500kg/m^3 (400m to 800m). The wave velocity was 1500m/s in ρ_1 and 3000m/s in ρ_2. In this test, it was emulated water and sedimentary rock, bringing the simulation closer to a realistic case.

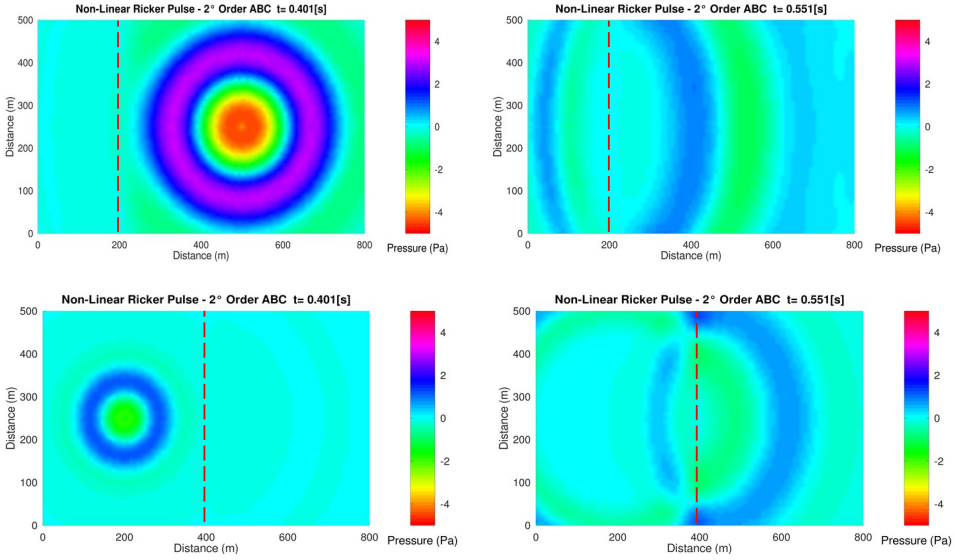

Figure 3. Non-linear acoustic wave propagation in a heterogeneous medium by layer. In the first case (a), we see the wave being generated in layer 2 (200m to 800m / ρ_2=2500kg/m³) and propagating through layer 1 (0m to 200m / ρ_1=1000kg/m³). In the second case (b), we see the wave being generated in layer 1 (0m to 400m / ρ_1=1000kg/m³) and propagating through layer 2 (400m to 800m / ρ_2=2500kg/m³).

In this third test, the phenomena of reflection and refraction of the acoustic wave due to the change of medium were observed. In both propagation directions, that is, from medium ρ_1 to ρ_2 or from ρ_2 to ρ_1, the reflection preserved the phase of the wave. Additionally, a decrease in the wavelength (λ) was observed when entering the less dense medium (smaller velocity) and an increase in λ when transitioning to the denser medium (bigger velocity), as predicted by theory. The second-order ABC demonstrated good absorption in both media.

Through test 4, it was possible to verify a higher efficiency of the second-order ABC method compared to the first-order one in absorbing acoustic waves in square meshes. The results of this test showed improved absorption by the second-order ABC due to its better handling of tangential components of the wave propagation vector, particularly in minimizing reflections at domain corners, as can be seen in Figure 4.

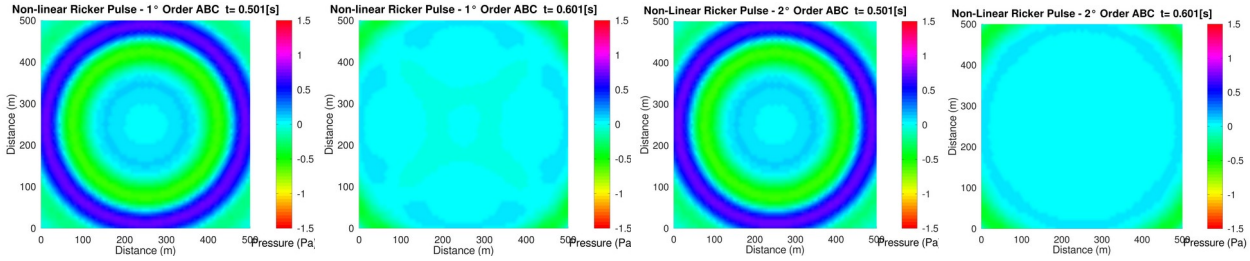

Figure 4. Non-linear acoustic wave propagation with 1st and 2nd order ABC (Absorbing Condition).

This difference in absorption can also be observed through the seismogram and the wave capture at a single point in the mesh at P=(140,250) over time (Figure 5).

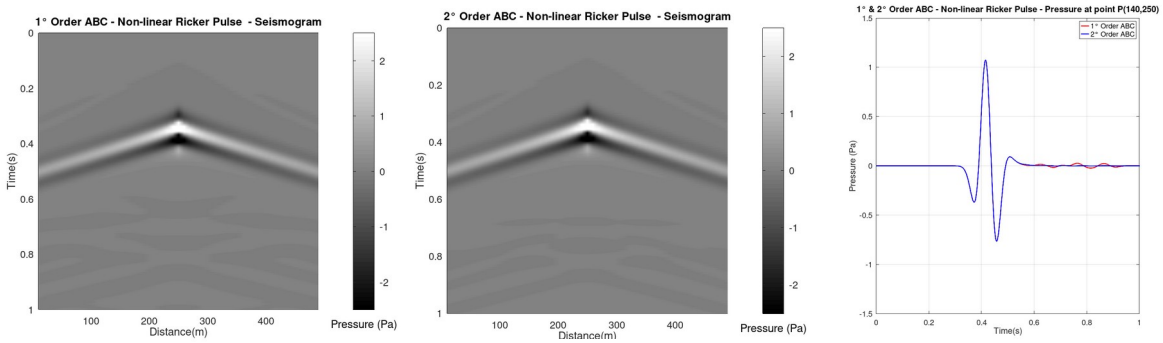

Figure 5. Seismogram of the non-linear Acoustic Wave with 1st and 2nd order ABC (a) (b). Comparison of the reflection over time at a fixed point (c).

In the final test, the nonlinear Acoustic Wave was propagated in a homogeneous circular mesh. The results showed a very similar performance between the first-order and second-order ABC boundary conditions (Figure 6). Unlike the square mesh, in a circular domain, the corner problem is automatically eliminated. This means that the term related to the tangential components of the wave vector, present in the second-order ABC formulation, does not have any influence in this case. With the source positioned exactly at the center of the domain, all wave rays reach the surface in a perfectly orthonormal manner. Thus, the absorption of the second-order ABC becomes close enough to that of the first-order ABC.

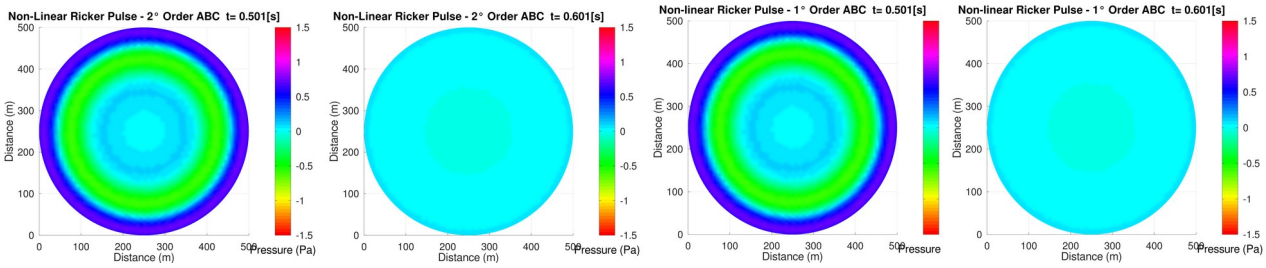

Figure 6. Non-linear acoustic wave propagation with 1st and 2nd order ABC (Absorbing Condition) at circular mesh.

6 Conclusions

The numerical implementation of the nonlinear acoustic wave equation by the finite element method was successful. The conservation of symmetry of the results after the P-wave reflects numerous times in a square geometry was verified using a mesh composed of non-uniform triangular elements, the same was verified if the geometry is circular. Since the pressure source has a maximum amplitude around unity, it is expected that the non-linear model of the present work behaves well with the results obtained by the linear model. In non-circular geometry, the second-order Absorbing Boundary Condition (ABC) is more effectiveness than the first-order one, radiating acoustic waves beyond the finite domain. This effectiveness is expected because the second-order formulation includes a term to treat components tangential to the boundary. In a circular mesh, the absence of

corners resulted in similar performance between first and second order ABCs. In this case, with the source in the center of the circle, the acoustic wave impacts perpendicularly to the boundary.

Acknowledgements. The authors would like to thank the local organizing committee, the Postgraduate Program in Environmental Engineering (PPGEA) at the Federal University of Espírito Santo, and the Fundação de Amparo à Pesquisa do Estado do Espírito Santo (FAPES), the Brazilian Postgraduate Agency.

Authorship statement. The authors hereby confirm that they are the sole liable persons responsible for the authorship of this work, and that all material that has been herein included as part of the present paper is either the property (and authorship) of the authors, or has the permission of the owners to be included here.

References

[1] Chacaltana, J. T. A. *et al*. Volumes Finitos não Estruturados voltado à Propagação de Ondas Acústicas em Meios Heterogêneos. *In:* PROCEEDINGS OF THE XLI IBERO-LATIN-AMERICAN CONGRESS ON COMPUTATIONAL METHODS IN ENGINEERING, Rio de Janeiro. **Anais…** Rio de Janeiro, CILAMCE, 2015.
[2] Peres, R. A. *et al. et al*. 1D Nonlinear Acoustic Wave Equation In Heterogeneous Fluid. *In:* PROCEEDINGS OF THE XLIV IBERO-LATIN-AMERICAN CONGRESS ON COMPUTATIONAL METHODS IN ENGINEERING, Porto. **Anais…** Porto, CILAMCE, 2023.
[3] Piccoli, F. P. *et al*. Nonlinear Acoustic Wave Propagation in Stratified Media. *In:* PROCEEDINGS OF THE XLI IBERO-LATIN-AMERICAN CONGRESS ON COMPUTATIONAL METHODS IN ENGINEERING, *41*, 2020, Foz de Iguaçu. **Anais…** Foz de Iguaçu, CILAMCE, 2020.
[4] Frasson, A. M. F. Simulação por Elemento Finitos 3D de problemas eletromagnéticos no tempo e na frequência. 196f. **Tese** (Doutorado), Programa de Pós- Graduação em Engenharia Elétrica, Faculdade de Engenharia Elétrica e da Computação da Universidade Estadual de Campinas, Universidade Estadual de Campinas, Campinas, 2002.
[5] Araujo, L. *et al.* Acoustic wave propagation in non-homogeneous media. In: PROCEEDINGS OF THE XLI IBERO-LATIN-AMERICAN CONGRESS ON COMPUTATIONAL METHODS IN ENGINEERING, 41, 2020, Foz de Iguaçu. **Anais**… Foz de Iguaçu, CILAMCE, 2020.
[6] Costa, E. S.; Medeiros, E. B. Estudo sobre a propagação acústica em águas rasas. *In:* CONGRESSO DE MÉTODOS NUMÉRICOS EM ENGENHARIA, Lisboa. **Anais…** Lisboa, 2015.
[7] Valente, A. et al. 3D OcTree Finite-volume method for acoustic wave simulation. In: PROCEEDINGS OF THE XLI IBERO-LATIN-AMERICAN CONGRESS ON COMPUTATIONAL METHODS IN ENGINEERING, 2015, Rio de Janeiro. **Anais**… Rio de Janeiro, CILAMCE, 2015.
[8] Neto, F. A. S. Modelagem acústica por diferenças finitas e elementos finitos em 2-D E 2,5-D. 123f. **Dissertação** (Mestrado), Programa de Pós- Graduação em Geofísica, Centro de Geociências, Universidade Federal do Pará, Pará, 2004.
[9] Campos-pozuelo, C. et al. Finite-element analysis of the nonlinear propagation of high-intensity acoustic waves. **Journal of Acoustic Society of America**, v. 106, n. 1, p. 92-101, 1999.
[10] Blackstock, D. T. On Plane, Spherical, and Cylindrical Sound Waves of Finite Amplitude in Lossless Fluids. New York: **Letters to the editor**, p. 217- 219, 1964.
[11] Beyer, R. T. **Nonlinear acoustics**. *In:* Physical Acoustics. New York: Academic, v. 2, p. 231–264, 1965.
[12] Lauterborn, *et al*. **Nonlinear Acoustic in Fluids**. *In:* Physical and Nonlinear Acoustic. Springer Handbook of Acoustics, part. B, p. 257-297, 2007.
[13] Pierce, A. D. **Acoustics: An Introduction to its Physical Principles and Applications**. Ed. 3. Springer Nature Switzarland, 2019.
[14] Garrett, S. L. **Understanding Acoustics: An Experimentalist's View of Sound and Vibration**. Ed. 2. Springer Nature Switzarland, 2020.
[15] Hamilton, M. F.; Blackstock, D. T. On the coefficient of nonlinearity in nonlinear acoustics. **Journal of Acoustic Society of America**, v. 86, n. 1, p. 74-77, 1987.
[16] Bamberger, A. *et al.* Second-order absorbing boundary conditions for the wave equation: a solution for the corner problem. **Siam. J. Numerical Analytical**, v. 27, n. 2, p. 323-352, 1990.
[17] Gholamy, A.; Kreinovich, V. Why Ricker Wavelets Are Successful in Processing Seismic Data: Towards a Theoretical Explanation. **Departmental Technical Reports (CS)**, v. 861, 2014.
[18] Wang, Y. The Ricker wavelet and the Lambert W function. **Geophys. J. Int**., v. 200, p. 111–115, 2015.
[19] Oden, J. T.; Fost, R. B. convergence, accuracy and stability of finite element approximations of a class of non-linear hyperbolic equations. **International Journal for Numerical Methods in Engineering**, v. 6, p. 357-365, 1973.